Chapter 11

The Antiproton, Proton, and Electron Mass Comparison

The Penning trap is a flexible device capable of comparing very different masses and particles of opposite charge. Nevertheless, possible systematic errors are minimized in a Penning trap by comparing mass doublets of a single charge polarity. With nearly the same charge to mass ratio the orbit sizes, particle location, and trap potential and polarity are similar. Examples of measurements on mass doublets of similar charge are comparisons of CO^+ and $N_2{}^+$ [21] and $^3He^+$ and $^3H^+$ [105,68]. More difficult comparisons are those involving very different masses and/or different sign of charge. An example of the former is a comparison of p^+ and e^- [50,53,98,99,100], and of the later is a comparison of e^+ and e^- [86]. As stressed in the last chapter, the major difficulty centers on being absolutely certain that the particles to be compared oscillate in the same magnetic field.

In this chapter we present a series of comparisons where we load and measure the cyclotron frequency of antiprotons and protons using our most recent techniques discussed in Chapters 7 and 9. The measurements are performed on small clouds of antiprotons or protons (typically 200 - 2000). These clouds both have the possibility of being contaminated with impurity ions that are very different (in one case electrons, in the other positively charged ions). As a check in our measurements we also compare both the antiproton and proton to the electron mass. The electron is relatively easy to study at the level of precision of our existing work and since the electron mass is very different from the antiproton mass,

it also provides an additional check of possible systematic effects. Our approach is to perform a self-consistent three way mass comparison each with a different variation of mass or charge polarity.

In Fig 11.1 we show a series of measurements of the cyclotron frequencies of antiprotons, protons, and electrons. We specifically analyze five sets of measurements where antiproton, proton, and electron cyclotron frequencies have each been measured. For comparing protons to electrons we extend the data to seven sets. This data represents only the most recent of several hundred antiproton frequency measurements and is chosen because all three particles were measured relatively close in time. The measurements use our most developed techniques to interrogate the particle motion with as little as heat as possible. Each measurement set is taken over an average time span of about 20 hours. Although the time to prepare a new particle species for a measurement is about one hour, we begin each measurement set with several measurements on a small antiproton cloud, then after ejecting the antiprotons, we prepare and measure electrons and protons as described in Chapters 6, 7, and 9. We complete a comparison set by again loading antiprotons and measuring their resonant frequencies.

Cyclotron measurements taken over the comparison time are shown in Fig. 11.1 and each data set used in subsequent analysis is identified. All antiprotons and proton measurements are performed at about $\pm$ 71 Volts by simultaneously observing the frequencies ν_c' and ν_z as described in Chapter 9. The electron measurements are taken with the axial frequency locked as described in Chapter 6.

The free space cyclotron frequency is determined by

$$(\nu_c)_i = (\nu_c')_i^2 + \frac{(\nu_z)_i^2}{2(\nu_c')_i}. \tag{11.1}$$

The uncertainty assigned to each point is the quadrature sum of the cyclotron and magnetron linewidths defined by

$$\sigma_i^2 \equiv (\Delta\nu_c')_i^2 + \left(\frac{\nu_z}{\nu_c'}(\Delta\nu_z)_i\right)^2. \tag{11.2}$$

For the antiproton and proton measurements, $\Delta\nu_c'$ and $\Delta\nu_z$ are the HWHM linewidths of the Fourier transform power spectrum (measured as 0.707 V_{rms}) of each frequency.

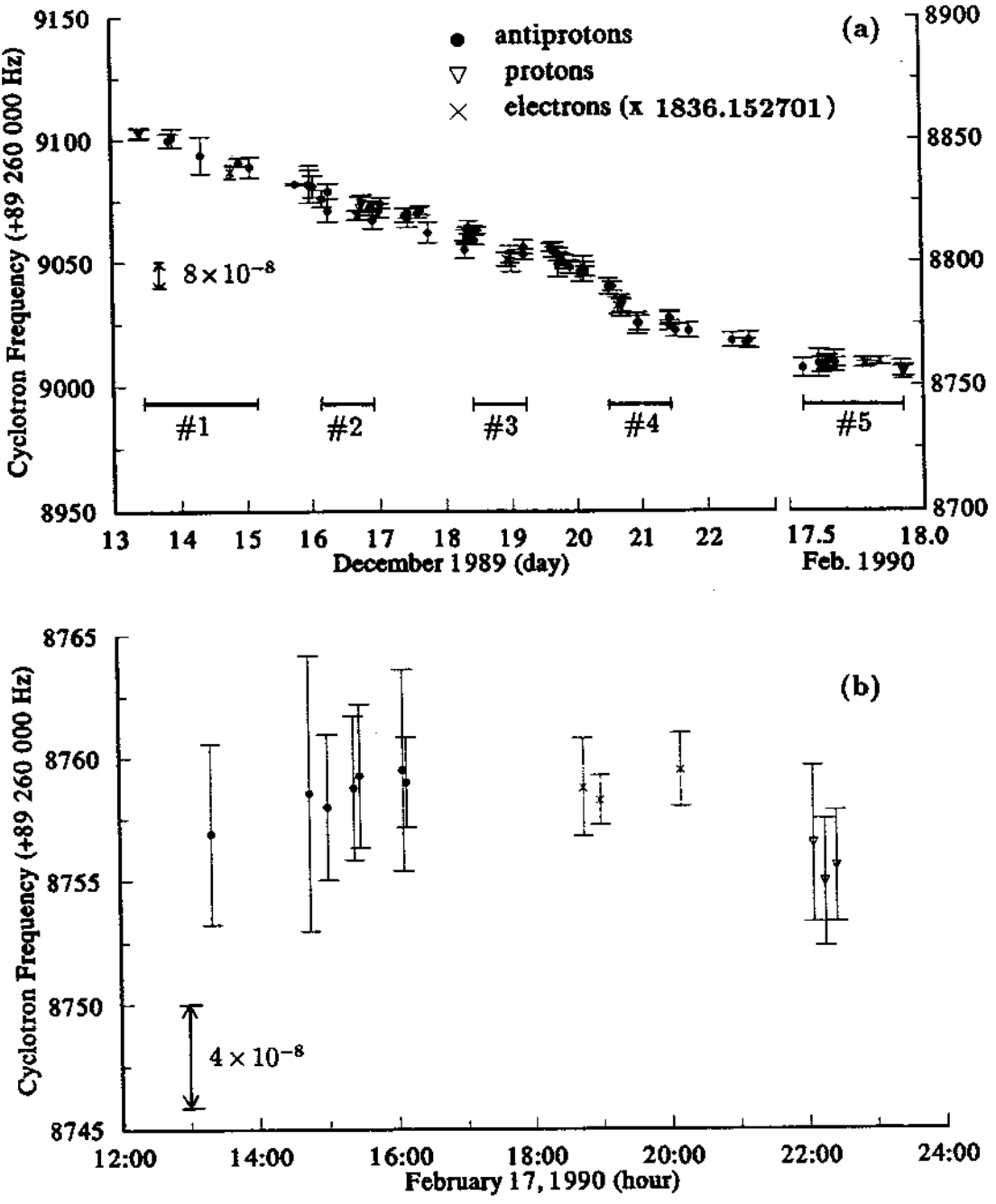

Figure 11.1: (a) Series of cyclotron measurements for antiprotons, protons and electrons over time. The 5 three way comparison sets are shown. (b) Expanded view of comparison set #5.

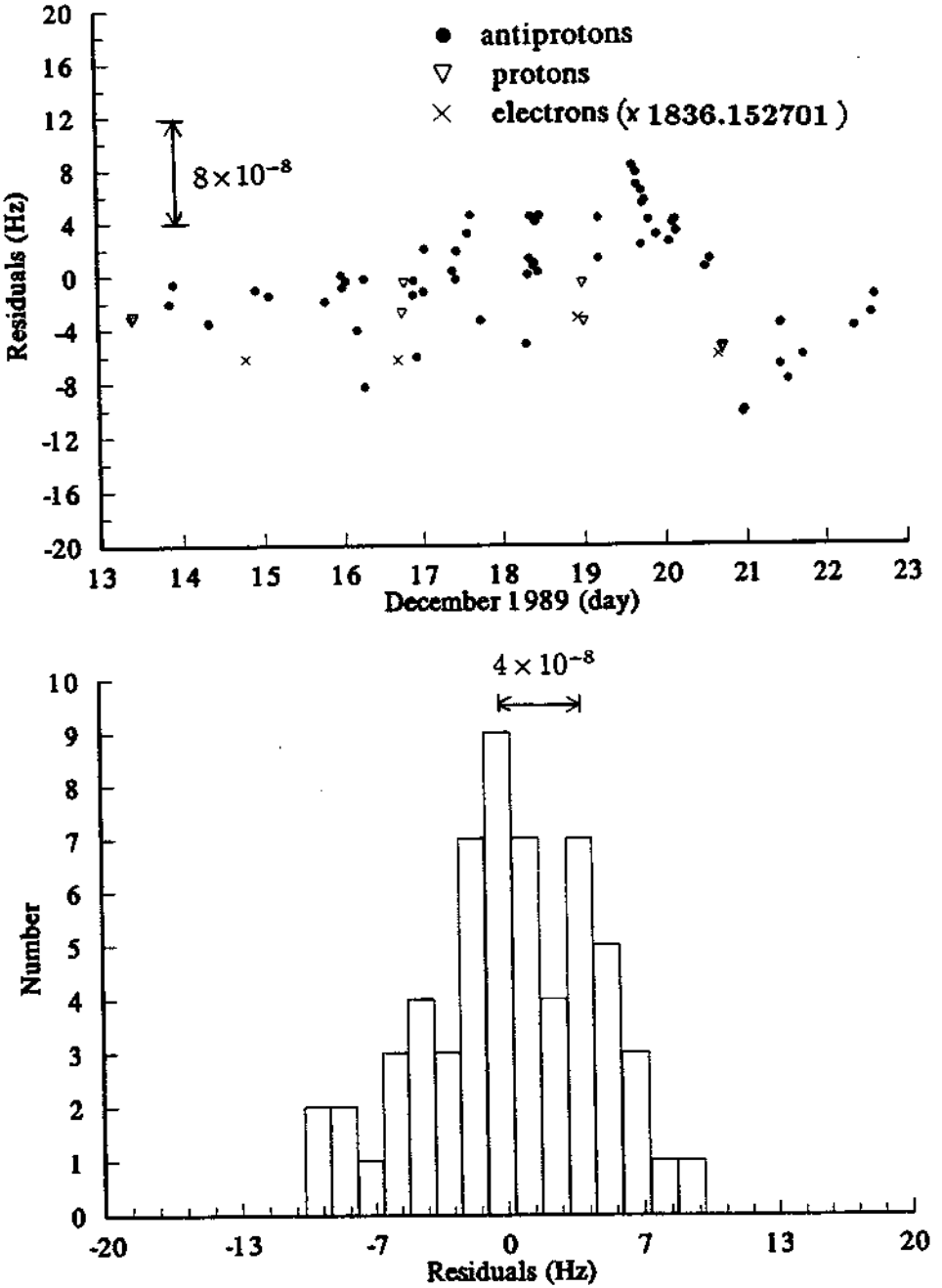

Figure 11.2: (a) The data in Fig. 10.1 with the magnetic field drift subtracted out. (b) The residuals about the least squares fit showing the scatter of the antiproton measurements taken over the 10 day period.

Table 11.1: Statistical Data of the 5 (and 7) Mass Comparison Sets.

Set		Time [hours]	Meas. # beg.	Meas. # end	$\overline{\nu_c}$ Mean	$\overline{\nu_c}$ Weighted	Standard Deviation [Hz] Scatter	Linewidth	Total
					89 269 000+				
	$\overline{p}$			3 2	218.81	219.25	1.75	1.19	2.11
1	e^-	40.6		1	(214.38)†			(2.80)	(3.30)
	p		2		217.36	217.37		1.43	2.26
	$\overline{p}$		3	3	217.33	219.52	3.22	1.39	3.50
2	e^-	17.7		1	(214.69)†			(1.63)	(3.61)
	p			2	218.61	218.94		2.77	4.25
	$\overline{p}$		3	2	224.23	224.31	2.71	0.81	2.82
3	e^-	18.8		1	(217.49)†			(2.72)	(3.84)
	p			3	221.61	222.11		2.15	3.45
	$\overline{p}$		2	4	215.74	216.90	3.65	1.01	3.78
4	e^-	22.4		1	(214.85)†			(3.27)	(4.90)
	p			4	217.26	217.32		1.49	3.94
					89 268 000+				
	$\overline{p}$		7		758.56	758.68	1.49	1.11	1.86
5	e^-	9.0		3	(758.84)†	(758.65)		(0.69)	(1.64)
	p			3	754.07	755.40		1.47	2.09
6	e^-	7.0		2	(638.45)†	(638.45)	1.16	(1.00)	(1.53)
	p		4		637.23	637.80	1.16	2.03	2.34
7	e^-	47	1		(633.4)†		0.90	(1.00)	(1.34)
	p			2	634.55	635.00		2.30	2.47

† To facilitate comparisons, $\nu_c[e^-]$ is tabulated as the nearly equivalent proton frequency $(m_e/m_p)\nu_c[e^-]$ using the ratio m_p/m_e=1836.152 701.

Table 11.2: Mass Ratio Weighted Averages and Uncertainties.

Antiproton / Proton

Set	$1-(m_{\bar{p}}/m_p)$	$\Delta(m_{\bar{p}}/m_p)$				
1	$+2.1\times10^{-8}$	3.5×10^{-8}	Average	=	1.3×10^{-8}	
2	$+0.65\times10^{-8}$	6.3×10^{-8}	Weighted average	=	2.3×10^{-8}	
3	$+2.5\times10^{-8}$	5.0×10^{-8}	σ_{scat}	=	1.6×10^{-8}	
4	-0.45×10^{-8}	6.1×10^{-8}	σ_{line}	=	1.9×10^{-8}	
5	$+3.7\times10^{-8}$	3.1×10^{-8}	σ_{sys}	=	2.0×10^{-8}	
			σ_{width}	=	2.8×10^{-8}	

Antiproton / Electron

Set	$m_{\bar{p}}/m_{e^-}$	$\Delta(m_{\bar{p}}/m_{e^-})$				
	1836.152...					
1	600	079	Average	=	1836.152 623	
2	601	101	Weighted Ave.	=	1836.152 648	
3	560	096	σ_{scat}	=	0.000 055	(3.0×10^{-8})
4	658	125	σ_{line}	=	0.000 035	(1.9×10^{-8})
5	700	050	σ_{sys}	=	0.000 037	(2.0×10^{-8})
			σ_{width}	=	0.000 050	(2.8×10^{-8})

Proton / Electron

Set	m_p/m_{e^-}	$\Delta(m_p/m_{e^-})$				
	1836.152...					
1	639	081				
2	613	113				
3	605	104	Average	=	1836.152 666	
4	658	127	Weighted Ave.	=	1836.152 693	
5	768	054	σ_{scat}	=	0.000 058	(3.2×10^{-8})
6	714	056	σ_{line}	=	0.000 027	(1.5×10^{-8})
7	668	057	σ_{sys}	=	0.000 037	(2.0×10^{-8})
			σ_{width}	=	0.000 050	(2.8×10^{-8})

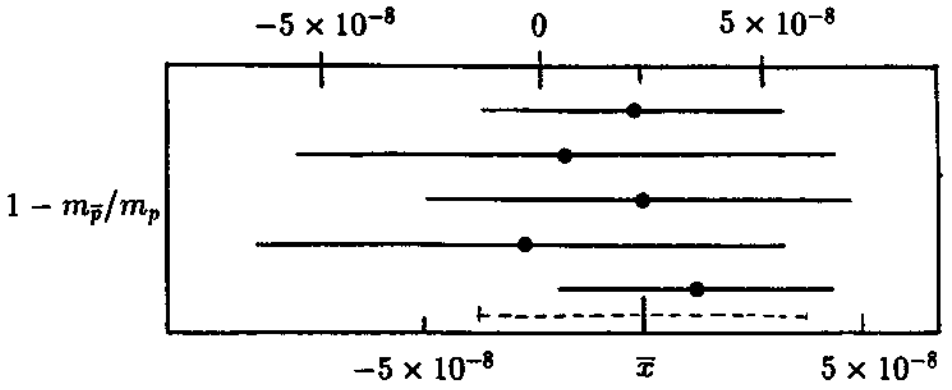

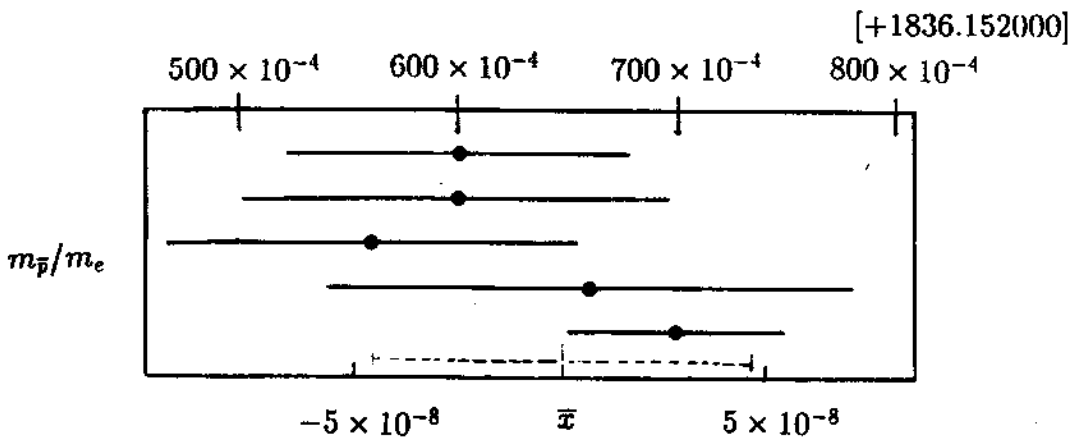

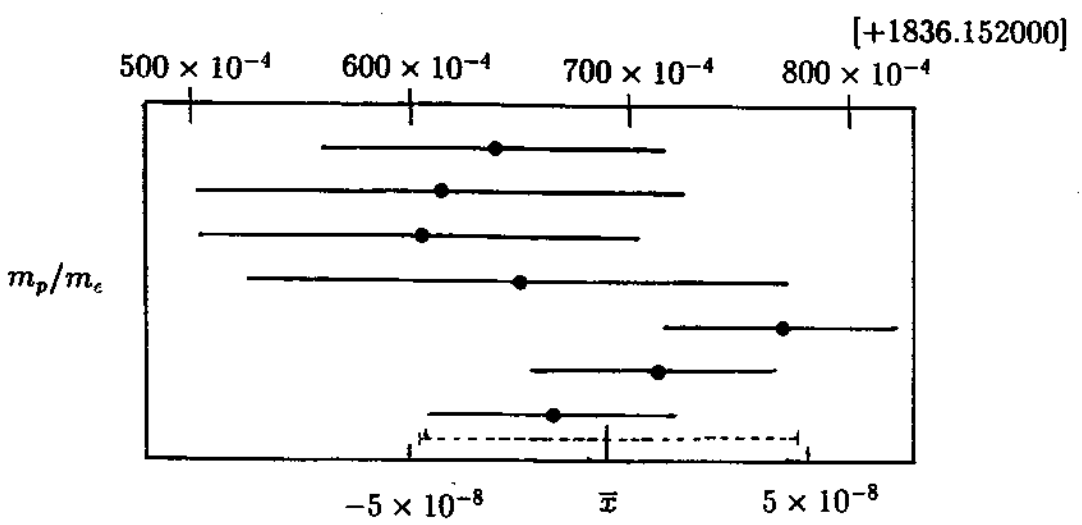

Figure 11.3: Mass comparisons $m_{\bar{p}}/m_p$, $m_{\bar{p}}/m_p$, and m_p/m_e-. The weighted average and assigned uncertainty is shown in dashed lines.

The points in Fig. 11.1 are plotted as a function of time. So that the measured electron cyclotron frequencies can be presented on the same scale, they are reduced by the high precision proton to electron mass ratio m_p/m_e=1836.152701 previously measured by R. VanDyck et al. [100,72]. This is for convenience only. All mass comparisons discussed and reported are completely independent of this earlier measurement.

For the first four data sets shown in Fig. 11.1 there exists a large drift in the magnetic field. This is a result of the magnet being energized and shimmed only a few days before this particular set of measurements were taken. In addition, a few of the points in the figure have been corrected for a field shift resulting from the S-5 bending magnet (see Fig. 3.10) being on or off. Of the five data sets, #3 and #5 were taken with the bending magnet off. This shift was carefully measured and was discussed in Chapter 10.

Since the magnet drift is so high for the first four data sets, it must be taken into account. To do this, we fit the antiproton points during the days of December 13-21 to a straight line. The assumption is made that the shifts due to small variations in cloud number and size are not significant on this scale and that the antiprotons can be used to map the magnetic field. In Fig. 11.2(a), we show the residuals of the points over the region that includes the first four data sets after subtracting the least squares fit. In Fig. 11.2(b) we show a histogram of all the antiproton data points in this region about the fit. The distribution of residuals represents the long term drift uncertainties and incorporates local fluctuations in the field that are in part responsible for the scatter of the points.

After correcting the data for the long term field drift each data set is then individually analyzed. Short term variations in the field drift are not subtracted out but are accounted for in the scatter of the points within a given data set calculated by

$$\sigma^2_{scat} \equiv \frac{\sum_{i=1}^{N}((\nu_c)_i - \overline{\nu_c})^2}{N-1}. \tag{11.3}$$

In Table 11.1 we show the summarized analysis of each data set (again for convenience, we tabulate the electron measurements by dividing $\nu_c(e^-)$ by 1836.152 701. For example, in data set #2, we have six antiproton measurements, three

at the beginning and three at the end of the set. One electron and two proton measurements were performed in between. The average and weighted average (where the associated weight of each measurement is the inverse of the variance $1/\sigma_i^2$) of the particle cyclotron frequencies are obtained respectively by

$$\overline{\nu}_c = \frac{1}{N}\sum_{i=1}^{N}(\nu_c)_i, \tag{11.4}$$

and

$$(\overline{\nu}_c)_w = \frac{\sum_{i=1}^{N}\frac{(\nu_c)_i}{\sigma_i^2}}{\sum_{i=1}^{N}\frac{1}{\sigma_i^2}}. \tag{11.5}$$

The values for $(\nu_c)_i$ and $(\sigma)_i$ are defined by Eq. 11.1 and Eq. 11.2. An assigned linewidth to each particle species in a given set is defined in terms of the individual linewidths by

$$\frac{1}{\sigma_{line}^2} \equiv \sum_{i=1}^{N}\frac{1}{\sigma_i^2}. \tag{11.6}$$

As suggested in contemporary literature on the subject of errors in precision measurements [74,90], each point is assigned with an associated uncertainty defined by

$$\sigma^2 \equiv \sigma_{scat}^2 + \sigma_{line}^2. \tag{11.7}$$

As seen in Table 11.1 much of the uncertainty is in the scatter over the relatively long comparison times within most data sets. Each data set is now represented by three measurements, one each for the antiproton, proton, and electron with weighted average $(\overline{\nu}_c)_w$ and associated uncertainty σ. In most cases the weighted average is similar to the average since measurement linewidths are nearly the same for most points.

We now take the mass ratios between each of the three points in a given measurement set and calculate an uncertainty from the two input uncertainties. The ratios 1-$(m_{\overline{p}}/m_p)$, $m_{\overline{p}}/m_{e^-}$, and m_p/m_{e^-} with the corresponding uncertainty are tabulated in Table 11.2 and plotted in Fig. 11.3. The average and weighted average are now taken over the five mass comparison sets (in the case of protons and electrons we use seven sets). The averages are calculated analogously to the earlier analysis and the weighted average over the data sets (Table 11.2) yield the

final mass ratio value. The uncertainty is determined by calculating the scatter of the 5 (or 7) points about the mean ratio value analogous to Eq. 11.3 except with the mean cyclotron frequency replaced by the mean of the ratio values. We also determine a 'linewidth' uncertainty σ_{line} using Eq 11.6 . The total uncertainty for each ratio measurement is defined by

$$\sigma^2 \equiv \sigma_{scat}^2 + \sigma_{line}^2 + \sigma_{sys}^2 + \sigma_{width}^2, \tag{11.8}$$

where σ_{sys} represents the 2×10^{-8} fractional systematic uncertainty and σ_{width} reflects our unwillingness to split the observed resonance lines as discussed in Chapter 10. The values for each of these error terms is tabulated in Table 11.2.

The weighted average of the ratio comparison gives the final measured result. The antiproton to proton mass ratio is measured to be

$$\left(\frac{m_{\overline{p}}}{m_p}\right)_w = 0.999\ 999\ 977(42). \tag{11.9}$$

Comparing the antiproton mass to the electron's yields the ratio

$$\left(\frac{m_{\overline{p}}}{m_{e^-}}\right)_w = 1836.152\ 648(89). \tag{11.10}$$

Comparing the proton mass to the electron's yields the ratio

$$\left(\frac{m_p}{m_{e^-}}\right)_w = 1836.152\ 693(88). \tag{11.11}$$

The weighted average and total uncertainty added in quadrature are included in Fig. 11.3 and denoted in dashed lines. These values differ a slight amount from our most recent published values [48] as a result of small differences in the analysis of the scatter. These insignificant differences are only about 5 parts in 10^9 or about 15% of the assigned uncertainty.

A few observations can be made from the data in Fig. 11.3. These data sets were taken over a relatively long time period. A correlation seems to exist in the scatter of the antiproton to electron and the proton to electron comparisons, but not in the antiproton to proton comparisons. This may suggest that the fluctuating variable observable in this scatter is in the electron measurements or in our interpretation of the observed electron cyclotron lineshape.